

Nonlocal electrodynamics of fluxons and nonlinear plasma oscillations in a distributed Josephson junction with electrodes of arbitrary thickness

G. L. Alfimov¹ and A. F. Popkov^{1,2}¹*Moscow Institute of Electronic Engineering, Zelenograd, Moscow, 124498, Russia*²*F.V. Lukin's Institute of Physical Problems, Zelenograd, Moscow, 103460, Russia*

(Received 27 February 2006; published 12 June 2006)

We considered a distributed Josephson junction formed by superconducting plates of arbitrary thickness in the case of high critical current density when Josephson penetration depth λ_j is less than London length λ_L . A nonlocal equation describing electrodynamics of such a junction in nondissipative approximation is derived. The soliton-like excitations of kink type (fluxons) and of breather type are studied. It is shown that the role of nonlocality is crucial for the dynamical properties of these entities: if the nonlocality is strong enough, fluxons can lose their mobility. Interactions between fluxons in the nonlocal model are studied. It is shown that for some interval of fluxon velocities and for some parameters of the junction the interactions are of solitonic type. Also the interaction may result in the emergence of a robust and long-living oscillating state of breather type. These states are studied separately using the approximation of the solution profile by one temporal Fourier harmonic.

DOI: [10.1103/PhysRevB.73.214512](https://doi.org/10.1103/PhysRevB.73.214512)

PACS number(s): 74.50.+r, 02.60.Nm, 74.25.Qt

I. INTRODUCTION

In the last decade much attention has been given to Josephson junctions with so-called *nonlocal electrodynamics*.¹⁻⁷ The distributed Josephson junction with nonlocal electrodynamics is a junction with high critical current j_s , large London screening length λ_L , small coherence length ξ and small Josephson penetration depth λ_j , where the relation $\xi \ll \lambda_j \ll \lambda_L$ holds. Here

$$\lambda_j = \sqrt{\frac{c\Phi_0}{16\pi^2\lambda_L j_s}}, \quad (1)$$

where c is the velocity of light and Φ_0 is the quantum of magnetic flux. For the first time nonlocal properties of the junction of such kind were discussed in Ref. 1 when considering a junction in thin superconductive film where the thickness of the superconductive layer d is far less than London screening depth in the material, $d \ll \lambda_L$. It was found that the magnetostatics of the junction becomes nonlocal due to the influence of the magnetic field outside the junction. Since the internal structure of the magnetic vortex in the nonlocal model differs essentially from the one for traditional electrodynamics, the dynamical properties of the magnetic vortex also change. Recently this theoretical prediction has been confirmed by experimental study of artificially fabricated Josephson junction of this kind.¹¹ It has been shown in Ref. 11 that in very narrow long Josephson junction the dependence of the magnetic vortex mass on the junction width is no longer linear and the corrections can be explained by taking into account nonlocal electrodynamics of the junction. Also the nonlocal electrodynamics has been derived for a system of magnetically coupled Josephson junctions,⁸⁻¹⁰ which can be described by coupled integrodifferential equations.

Nonlocal Josephson electrodynamics appears in a natural way when describing weak links inside high- T_c superconductors.^{2,3} The nonideal crystalline structure of the superconductor includes extensive defects of packing, grain boundaries, and other imperfections which reduce locally the

depairing current.¹² Such defects of the crystalline lattice can be treated as natural weak links. The role of the weak links is especially important for $\text{YBa}_2\text{Cu}_3\text{O}_{7-\delta}$ superconductors.^{13,14} In these superconductors the magnitude of the local depairing current j_b at the grain boundaries is very sensitive to the misorientation angle and can vary from the bulk depairing current j_d to very small values $j_b \ll j_d$.^{13,15,17} These facts follow from the general theory of the Josephson effect in anisotropic superconductors with d -wave symmetry.¹⁸ According to Ref. 19, the variation of HTS crystal orientation at the junction changes both the critical current and sin-like dependence of the supercurrent versus the phase jump on the junction. When the temperature is not too low this dependence remains nearly harmonic (sin-like) whereas the range of the critical current variation is quite significant. Experimentally this theory was confirmed by several papers where temperature and field features of critical currents of HTS Josephson junctions were studied (see, e.g., Ref. 20), including ones on bi-crystal substrate (see Ref. 21). It seems quite attractive to investigate also the dynamical properties of such a superconducting junction connected with nonlocal electrodynamics.

As the misorientation angle decreases the local description fails and the magnetic vortices inside the weak link should be described by the nonlocal model. In this model the vortices pinned on the weak link approach in shape Abrikosov vortices with Josephson cores (AJ vortices). Correspondingly, the energy, mass and viscosity of the vortex change. This results in change of both the critical magnetic field for penetration of magnetic flux into the superconductor along the weak links²² and the general critical current, associated with the motion of the vortices along the weak links.^{13,15} Also the frequency spectrum of plasma oscillations in the junction changes in the short wavelength region.¹⁶ Recent experimental study of high- T_c superconductors¹³ has confirmed these theoretical predictions.

A significant part of theoretical studies of nonlocal Josephson junctions concerns dynamics of magnetic vortices. In particular, the steady motion of vortices and multi-vortex

states in nonlocal Josephson junction has been discussed.^{23–25} It has been shown that besides the traditional 2π kinks, quite rapid 4π kinks of various shape can appear in the nonlocal junction.^{23,26} The spectra of linear oscillations in the Josephson junction has been studied also, both in presence of magnetic vortices²⁷ or without it.¹⁶ However, many issues related to the nonlocal electrodynamics of the Josephson junctions remain unclear. One of them is the *mobility* of fluxons and multi-fluxon states. It was shown²⁶ that in non-dissipative approximation the traditional 2π -kinks can lose the mobility. This statement has been made based on the mathematical study of an idealized model, so it seems natural to verify this fact by means of numerical simulations. Another important issue is the *presence of long-lived oscillating states* of breather type. In traditional Josephson electrodynamics these objects are as fundamental as the fluxons and correspond to envelope solitons of the phase oscillations.^{28,29} So, the study of nonstationary dynamics of fluxons and such oscillatory states is important for understanding of nonlinear dynamics of Josephson junctions in general and for the description of the mechanism for magnetic flux penetration into the superconductor.³⁰ In the present paper some of these problems are discussed.

Our analysis is based on a nonstationary and nondissipative equation for the nonlocal Josephson junction with superconductive leads of arbitrary thickness. We deduce this equation in Sec. II. Similar equations have been derived before,^{2–4,31} including also dissipation.^{32,33} In these papers the resulting equations have been derived starting from stationary London equations and neglecting the displacement currents inside the junction leads. At the same time the validity of these assumptions needs some discussion. Specifically, it is known that if the frequency of electromagnetic oscillations is high enough, the superconducting leads become transparent for electromagnetic field. There are two mechanisms which cause this phenomenon. On the one hand, when the frequency of electromagnetic oscillations becomes comparable with the frequency of the superconductive gap, the order parameter sharply decreases. In the case of high- T_c superconductors this occurs for higher frequencies than in the case of low- T_c superconductors. Moreover, the London screening length λ_L in high- T_c superconductors is also greater than that in low- T_c superconductors. On the other hand, when taking into account the displacement currents in the junction leads, the London screening length λ_L should be renormalized. Both these points impose some restrictions for the frequencies of electromagnetic oscillations which can be described by the model. We show that the first mechanism is more restrictive than the second one and we estimate the interval of frequencies where the model remains valid.

The paper is organized as follows. In Sec. II we deduce a nonstationary equation to describe the nonlocal electrodynamics of the Josephson junction with superconductive leads of arbitrary thickness. We found the conditions when this nonlocal equation is applicable and we show that these conditions are different for steadily moving vortices and for oscillating breather-like objects. Section III is devoted to the mobility of fluxons in a nonlocal junction and their interaction with each other. It is shown that collisions of two fluxons can result in long-lived breather-like pulsating objects.

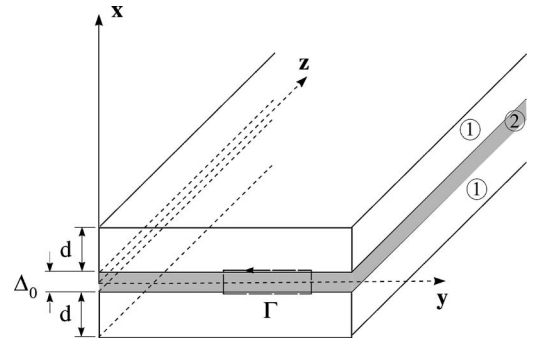


FIG. 1. Scheme of a Josephson junction: 1—superconductor, 2—tunnel layer.

Section IV is devoted completely to the breather-like objects. The results of numerical simulations are reported and the conditions for the existence and the stability of these entities are discussed. Section V contains a summary and discussion.

II. BASIC EQUATIONS AND MODEL ASSUMPTIONS

Let us consider a distributed Josephson junction (see Fig. 1) formed by two superconductive electrodes. Let Ψ be the wave function of the condensate of superconductive electrons, $\Psi = \Psi_0 \exp(i\theta)$. We assume that the amplitude Ψ_0 is a constant inside the electrodes (the “stiff wavefunction” assumption). This assumption is valid if the coherence length ξ inside the electrodes is small, $\xi \ll \lambda_L, \lambda_J$, where λ_L and λ_J are the London penetration depth and Josephson length correspondingly. In this case the temporal frequencies of currents and fields inside the leads should lie far from the superconductive gap Δ_c . This implies that

$$\omega \ll \Delta_c = \frac{k_B T_c}{\hbar} \quad (2)$$

where T_c is the temperature of the junction. In the case of high- T_c superconductor (e.g., YBiBaCu), where $T_c \sim 100$ K, Eq. (2) yields the condition $\omega \ll \Delta_c \sim 10^{13} \text{ s}^{-1}$. The electric (\mathbf{E}) and magnetic (\mathbf{H}) fields inside the superconductive layers are related to the current \mathbf{J} by means of the London’s equations

$$\mathbf{E} = \frac{4\pi\lambda_L^2}{c^2} \frac{\partial \mathbf{J}}{\partial t}, \quad (3)$$

$$\mathbf{H} = -\frac{4\pi\lambda_L^2}{c} \text{rot } \mathbf{J}, \quad (4)$$

where c is the velocity of light. After elimination of the current \mathbf{J} , Eqs. (3) and (4) are equivalent to one of the Maxwell equations, $\text{rot } \mathbf{E} = -\frac{1}{c} \frac{\partial \mathbf{H}}{\partial t}$. It follows from the second Maxwell equation,

$$\text{rot } \mathbf{H} = \frac{4\pi}{c} \mathbf{J} + \frac{\varepsilon}{c} \frac{\partial \mathbf{E}}{\partial t}, \quad (5)$$

and formulas (3) and (4) that the currents inside the superconductors satisfy the equation

$$\Delta \mathbf{J} - \nabla(\nabla \mathbf{J}) - \frac{1}{\lambda_L^2} \mathbf{J} = \frac{\varepsilon}{c^2} \frac{\partial^2 \mathbf{J}}{\partial t^2} \quad (6)$$

(here ε is the permittivity of the junction). The right-hand side term in Eq. (6) corresponds to the displacement currents inside the superconductive leads, the term $\frac{\varepsilon}{c} \frac{\partial \mathbf{E}}{\partial t}$ in Maxwell equation (5). It can be neglected if temporal frequencies of currents and fields inside the leads satisfy the relation

$$\omega \ll \frac{c}{\lambda_L \sqrt{\varepsilon}}.$$

Assuming that $c=3 \times 10^8$ m/s, $\lambda_L=0.1$ μm , and $\varepsilon \sim 10$, one has $\omega \ll 10^{15}$ s $^{-1}$. This condition is weaker than (2). Nevertheless, as we show below, this condition leads to some additional restrictions for the junction parameters for which the developed model is applicable.

Due to the ‘‘stiff wave function’’ assumption the superconductive current \mathbf{J}_i in i th electrode is related to the phase θ_i of the wave function Ψ_i and vector potential of the magnetic field \mathbf{A} , $\text{rot } \mathbf{A} = \mathbf{H}$, by the well-known relation

$$\mathbf{J}_i = \frac{c\Phi_0}{8\pi^2\lambda_L^2} \nabla \theta_i - \frac{c}{4\pi\lambda_L^2} \mathbf{A}. \quad (7)$$

Consider the Cartesian coordinates (x, y, z) . The plane $x=0$ coincides with the plane of symmetry of the junction (see Fig. 1). In order to deduce the boundary conditions we assume that the thickness Δ_0 of the oxide layer is small. Also we admit that the screening currents at both sides of the junction are antisymmetric to each other, i.e., $J_{y,1}(x=\frac{\Delta_0}{2}) = -J_{y,2}(x=-\frac{\Delta_0}{2})$. Then, integrating Eq. (7) along the contour Γ shown in Fig. 1 yields

$$\begin{aligned} J_y(x=+0) &= \frac{1}{2} \left[J_{y,1} \left(x = \frac{\Delta_0}{2} \right) - J_{y,2} \left(x = -\frac{\Delta_0}{2} \right) \right] \\ &= \frac{c\Phi_0}{16\pi^2\lambda_L^2} \frac{\partial(\theta_1 - \theta_2)}{\partial y} \\ &\quad - \frac{c}{8\pi\lambda_L^2} \left[A_y \left(x = \frac{\Delta_0}{2} \right) - A_y \left(x = -\frac{\Delta_0}{2} \right) \right]. \end{aligned} \quad (8)$$

The last term in Eq. (8) is of the order of Δ_0/λ_L and can be neglected. We arrive at the first boundary condition for the current,

$$J_y(x=+0) = \frac{c\Phi_0}{16\pi^2\lambda_L^2} \frac{\partial \varphi}{\partial y}, \quad (9)$$

where $\varphi \equiv \theta_1 - \theta_2$. The second boundary condition for the x component of the current follows from the fact that the complete perpendicular current is a sum of the superconductive component and the bias current,

$$J_x(x=+0) = J_x(x=-0) = j_s \sin \varphi + \frac{\varepsilon}{4\pi} \frac{\partial E_x}{\partial t}. \quad (10)$$

Taking into account the second Josephson equation,

$$E_x(x=0) = \frac{\Phi_0}{2\pi c \Delta_0} \frac{\partial \varphi}{\partial t},$$

we arrive at the relation

$$J_x(x=+0) = j_s \sin \varphi + \frac{\varepsilon\Phi_0}{8\pi^2 c \Delta_0} \frac{\partial^2 \varphi}{\partial t^2}. \quad (11)$$

If no external magnetic field is applied, the screening currents at the external boundaries $x=\pm d$ of the electrodes vanish, i.e.,

$$J_{x,y}(|x|=d) = 0. \quad (12)$$

In order to deduce the evolution equation for the phase jump of the wave function at the junction, $\varphi(y, t)$, we employ an approach similar to one used in Refs. 2, 4, 22, and 31. The current \mathbf{J} can be represented using the Fourier transform with respect to y and t :

$$\mathbf{J}(x, y, t) = \frac{1}{(2\pi)^2} \int_{-\infty}^{+\infty} e^{iky} dk \int_{-\infty}^{+\infty} \mathbf{J}^{k,\omega}(x) e^{-i\omega t} d\omega. \quad (13)$$

Solving vector equation (6) with boundary conditions (12) one obtains the following relation for the Fourier transforms of the components of the current ($J_{x,y} \neq 0$, $J_z = 0$):

$$\begin{aligned} J_x^{k,\omega}(x) &= \frac{ik\lambda_L^2}{1+k^2\lambda_L^2 - \varepsilon\omega^2\lambda_L^2/c^2} \frac{\partial J_y^{k,\omega}(x)}{\partial x} \\ &= -J_y^{k,\omega}(x) \frac{ik\lambda_L}{\sqrt{1+k^2\lambda_L^2 - \varepsilon\omega^2\lambda_L^2/c^2}} \\ &\quad \times \tanh\left(\frac{(d-|x|)\sqrt{1+k^2\lambda_L^2 - \varepsilon\omega^2\lambda_L^2/c^2}}{\lambda_L}\right) \end{aligned} \quad (14)$$

Taking into account relations (9), (11), and (14) for the longitudinal and transverse currents at $x=0$, after an inverse Fourier transform one arrives at the equation

$$\begin{aligned} \sin \varphi + \omega_0^{-2} \frac{\partial^2 \varphi}{\partial t^2} &= \frac{\omega_1 \lambda_J^2}{\lambda_L} \int_{-\infty}^{\infty} \int_{-\infty}^{\infty} \\ &\quad \times G_\beta \left(\frac{|y-u|}{\lambda_L}, \frac{c|t-\tau|}{\lambda_L \sqrt{\varepsilon}} \right) \frac{\partial^2 \varphi}{\partial u^2} du d\tau. \end{aligned} \quad (15)$$

Here

$$\omega_0^2 = \frac{8\pi^2 j_s \Delta_0 c}{\varepsilon \Phi_0} = \frac{c^2 \Delta_0}{2\varepsilon \lambda_J^2 \lambda_L}, \quad \omega_1 = \frac{c}{\lambda_L \sqrt{\varepsilon}},$$

and the kernel of the convolution operator is

$$\begin{aligned} G_\beta(\zeta, \eta) &= \frac{1}{(2\pi)^2} \int_{-\infty}^{\infty} \exp(i\tilde{k}\zeta) d\tilde{k} \int_{-\infty}^{\infty} \frac{\tanh(\beta\sqrt{1+\tilde{k}^2 - \tilde{\omega}^2})}{\sqrt{1+\tilde{k}^2 - \tilde{\omega}^2}} \\ &\quad \times \exp(-i\tilde{\omega}\eta) d\tilde{\omega}, \end{aligned} \quad (16)$$

where $\beta=d/\lambda_L$, $\tilde{k}=k\lambda_L$, and $\tilde{\omega}=\omega/\omega_1$. If the temporal frequencies lie around ω_0 , i.e., $\omega \sim \omega_0$, and if $\tilde{\omega} \sim \omega_0/\omega_1 = \sqrt{\Delta_0 \lambda_L}/\lambda_J^2 \ll 1$, then one can neglect the time dependence

in the integral term in (15). This is equivalent to neglecting the temporal dependence in Eq. (6) discussed above. This approximation is valid if

$$\Delta_0 \ll \frac{\lambda_J^2}{\lambda_L}. \quad (17)$$

In this case Eq. (15) can be replaced by a simple one:

$$\sin \varphi + \omega_0^{-2} \frac{\partial^2 \varphi}{\partial t^2} = \frac{\lambda_J^2}{\lambda_L} \int_{-\infty}^{\infty} G_\beta \left(\frac{|y-u|}{\lambda_L} \right) \frac{\partial^2 \varphi}{\partial u^2} du, \quad (18)$$

where

$$G_\beta(\zeta) = \frac{1}{2\pi} \int_{-\infty}^{\infty} \frac{\tanh(\beta\sqrt{1+k^2})}{\sqrt{1+k^2}} \exp(ik\zeta) dk. \quad (19)$$

Let us normalize t and y by $[t] = \omega_0^{-1}$ and $[y] = \lambda_J$, correspondingly, and define $\mu = \lambda_L/\lambda_J$. Then Eq. (18) can be rewritten in more a compact form that includes the two parameters β and μ only:

$$\sin \varphi + \frac{\partial^2 \varphi}{\partial t^2} = \frac{1}{\mu} \int_{-\infty}^{\infty} G_\beta \left(\frac{|y-u|}{\mu} \right) \frac{\partial^2 \varphi}{\partial u^2} du \equiv L_{\mu,\beta}[\varphi]. \quad (20)$$

Here we introduce the Fourier multiplying operator $L_{\mu,\beta}$, which has the symbol

$$\hat{L}_{\mu,\beta}(k) = - \frac{k^2 \tanh(\beta\sqrt{1+\mu^2 k^2})}{\sqrt{1+\mu^2 k^2}}. \quad (21)$$

It worth mentioning some limit cases of Eq. (20):

(a) $\mu \ll 1$. In this case the Fourier symbol (21) can be approximately replaced by

$$\hat{L}_{\mu,\beta}(k) \sim -k^2 \tanh(\beta)$$

and Eq. (20) transforms into the sine-Gordon equation with renormalized screening depth

$$\sin \varphi + \frac{\partial^2 \varphi}{\partial t^2} = \lambda_{eff}^2 \frac{\partial^2 \varphi}{\partial y^2}, \quad \lambda_{eff} = \sqrt{\tanh \beta}. \quad (22)$$

This limit corresponds to the traditional Josephson electrodynamics.

(b) $\beta \ll 1$. In this case expanding the Fourier symbol (21) for small β one arrives at

$$\hat{L}_{\mu,\beta}(k) = - \frac{k^2 \tanh(\beta\sqrt{1+\mu^2 k^2})}{\sqrt{1+\mu^2 k^2}} \sim -\beta k^2$$

and the equation becomes again the sine-Gordon one:

$$\sin \varphi + \frac{\partial^2 \varphi}{\partial t^2} = \beta \frac{\partial^2 \varphi}{\partial y^2}. \quad (23)$$

(c) $\beta \rightarrow \infty$. This is the case of ‘‘infinitely thick’’ superconductive electrodes. In this case the equation (20) transforms into the equation

$$\sin \varphi + \frac{\partial^2 \varphi}{\partial t^2} = \frac{1}{\pi\mu} \int_{-\infty}^{\infty} K_0 \left(\frac{|y-u|}{\mu} \right) \frac{\partial^2 \varphi}{\partial u^2} du \quad (24)$$

derived in Refs. 2–4.

In some situations the condition (17) for the applicability of Eq. (20) can be replaced by the condition $\Delta_0 \ll \lambda_L$. This restriction is weaker than (17), since in the nonlocal case $\lambda_J \ll \lambda_L$. As an example, let us consider the propagation of a wave of constant profile (e.g., fluxon) and velocity v , when $\varphi(y, t) = \varphi(y - vt)$. The Fourier transforms of the current can be rewritten in the form

$$\mathbf{J}^{k,\omega}(x) = \mathbf{J}^k(x) \delta(\omega - vk), \quad (25)$$

where $\mathbf{J}^k(x)$ is the Fourier transform of the current with respect to the travelling coordinate $\tilde{y} = y - vt$,

$$\mathbf{J}^k(x) = \frac{1}{2\pi} \int_{-\infty}^{\infty} \mathbf{J}(x, \tilde{y}) e^{ik\tilde{y}} dk.$$

Normalizing the spatial coordinate by $[\tilde{y}] = \lambda_J \sqrt{1 - \varepsilon^2 v^2/c^2}$ and using (14) and (25) one arrives at

$$(1 - \tilde{v}^2 \gamma^2) \sin \varphi + \tilde{v}^2 \frac{\partial^2 \varphi}{\partial \tilde{y}^2} = \frac{1}{\mu} \int_{-\infty}^{\infty} G_\beta \left(\frac{|\tilde{y}-u|}{\mu} \right) \frac{\partial^2 \varphi}{\partial u^2} du. \quad (26)$$

Here

$$\tilde{v} = \frac{v}{\lambda_J \omega_0}; \quad \gamma = \sqrt{\frac{\Delta_0}{2\lambda_L}}.$$

If $\Delta_0 \ll \lambda_L$ then $\tilde{v}\gamma \ll 1$ and Eq. (26) coincides with Eq. (20) for the solutions of the traveling wave type.

Equation (20) is the basic equation for the analysis in the rest of this paper.

III. FLUXONS IN DISTRIBUTED JOSEPHSON JUNCTIONS WITH NONLOCAL ELECTRODYNAMICS

A fluxon is a wave of the flip-over of the phase jump at the junction. From mathematical viewpoint a fluxon corresponds to the 2π kink (antikink) solution of the equation for the phase jump [Eq. (20), in our case]. For the junction with traditional electrodynamics this equation is the sine-Gordon one. It is well known that in the sine-Gordon case 2π kinks are robust and restore their shapes and velocities after interaction (solitonic interaction). This occurs due to complete integrability of the sine-Gordon equation.²⁹ In the junction with nonlocal electrodynamics the governing equation is no longer integrable and 2π kinks lose the solitonic properties. Moreover, even the existence of the travelling kink needs special investigation. It has been shown²⁶ that switching from the local to the nonlocal model can lead to the phenomenon of *discretization* of kink velocities. Below we summarize some analytical results on 2π kinks for Eq. (20) (Sec. III A), set out the results of numerical investigation for free propagation of travelling fronts of 2π -kink type (Sec. III B), and report on numerical simulation of their interactions (Sec. III C).

A. Analytical results

From the mathematical viewpoint the moving $2k\pi$ kinks of constant profile described by Eq. (20) satisfy the equation

$$\sin \varphi + v^2 \frac{d^2 \varphi}{d\xi^2} = \frac{1}{\mu} \int_{-\infty}^{\infty} G \left(\frac{|\xi - \eta|}{\mu} \right) \frac{d^2 \varphi}{d\eta^2} d\eta \quad (27)$$

with $G(\eta) = G_\beta(\eta)$ and with the boundary conditions

$$\lim_{\xi \rightarrow -\infty} \varphi(\xi) = 0; \quad \lim_{\xi \rightarrow +\infty} \varphi(\xi) = 2k\pi. \quad (28)$$

Here v is the $2k\pi$ -kink velocity and $\xi = y - vt$. If the kernel $G(\eta)$ is of the form

$$G(\xi) = \sum_{j=1}^N \kappa_j e^{-\eta_j |\xi|}, \quad \eta_j > 0, \quad \kappa_j > 0, \quad j = 1, 2, \dots, N \quad (29)$$

[(E) kernel, in terms of Ref. 26] then the following statements holds:

*Statement:*²⁶ Let the kernel $G(\xi)$ be of (E) type and $v > 0$. For $v = v^*$ let there exist a kink solution of (27) of the symmetry $\varphi(\xi) + \varphi(-\xi) = 2k\pi$, of topological charge k . Then, generically, there are no kink solutions of the same topological charge with velocity $v \in (v^* - \epsilon, v^* + \epsilon)$ for several value of $\epsilon > 0$.

The word “generically” implies some transversality condition. It is shown in Ref. 26 that the existence of $2k\pi$ kink with symmetry $\varphi(\xi) + \varphi(-\xi) = 2k\pi$ is a phenomenon of codimension 1 in the space of parameters $v, \kappa_j, \eta_j, j = 1, \dots, N$. So, fixing all these parameters except the velocity v , one can expect that these entities can exist for some isolated values of v . The existence of $2k\pi$ kink without this symmetry is a phenomenon of codimension 2 and hardly can be expected, if the parameters of the kernel $\kappa_j, \eta_j, j = 1, \dots, N$, are fixed. It was suggested in Ref. 26 that this phenomenon (called *discretization of kink velocities*) takes place not only for (E) kernels, but in a more general case also. In particular, numerical calculations shows that it takes place for kink solutions of Eq. (24). It was shown also in Ref. 26 that in the case $v = 0$ a degeneration occurs and the existence of $2k\pi$ kink becomes a phenomenon of codimension 0 in the space of parameters $\kappa_j, \eta_j, j = 1, \dots, N$. So, the existence of at-rest $2k\pi$ kink is in some sense “more probably” that the existence of the kink with any other velocity.

Returning to the kernel $G_\beta(\xi)$, one can rewrite it in the form of the following series:²²

$$G_\beta(\xi) = \frac{1}{\beta} \sum_{n=0}^{\infty} \frac{\exp \left[- \sqrt{1 + \left(\frac{\pi}{2\beta} \right)^2 (1 + 2n)^2} |\xi| \right]}{\sqrt{1 + \left(\frac{\pi}{2\beta} \right)^2 (1 + 2n)^2}}. \quad (30)$$

So, by truncating the expansion (30), the kernel $G_\beta(\xi)$ can be approximated by (E) kernels with arbitrary accuracy. One can expect that Eq. (27) with the kernel $G_\beta(\xi)$ inherits the features of the model with (E) kernels and the phenomenon of discretization of kink velocities takes place in this case also. Since there is no rigorous proof of this statement we formulate it as a conjecture as follows:

Conjecture 1: For any value of μ the velocities of the $2k\pi$ kinks described by Eq. (27) with the boundary conditions (28) and $G(\eta) = G_\beta(\eta)$ are isolated. This means that if $v^* \neq 0$ is a velocity of some $2k\pi$ kink solution of Eq. (27), then there exists an interval $(v^* - \epsilon; v^* + \epsilon)$ for some $\epsilon > 0$ such that there is no other $2k\pi$ kink solution with velocity v within this interval.

The discretization of kink velocities contrasts with traditional (local) description of the Josephson junction based on the sine-Gordon model, where there exists a *continuous set* of 2π -kink velocities. Moreover, the results of our numerical analysis of Eq. (27) with $G(\eta) = G_\beta(\eta)$ and boundary conditions (28) for the solution of 2π -kink type allows one to put forward a stronger hypothesis:

Conjecture 2: There is no solution of Eq. (27) with the boundary conditions (28) and $G(\eta) = G_\beta(\eta)$ with $v \neq 0$.

In the case $v = 0$ the 2π kinks can be found numerically (see Ref. 22).

B. The propagation of 2π kink: Numerical analysis

Evidently, the approximation (27) and (28) is very restrictive for physical applications. It corresponds to the idealized situation when a strictly localized fluxon moves without any change of its form in infinitely long Josephson contact. At the same time one can expect that in the limit when the governing equation (20) can be approximately replaced by the sine-Gordon one it should describe traveling 2π fronts of nearly constant shape. In particular,

(a) if $\mu \ll 1$ Eq. (20) can be replaced by Eq. (22), which admits traveling 2π -kink (antikink) solution,

$$\varphi(t, y) = 4 \arctan \left[\exp \left(\pm \frac{y - vt}{\sqrt{\tanh \beta - v^2}} \right) \right].$$

(b) If $\beta \ll 1$, the dynamics can be described approximately by Eq. (23). The 2π -kink solution of this equation is

$$\varphi(t, y) = 4 \arctan \left[\exp \left(\pm \frac{y - vt}{\sqrt{\beta - v^2}} \right) \right],$$

which exist for small values of velocity $v^2 < \beta$.

In order to study the dynamics described by (20), the following numerical experiments have been fulfilled. We have used the profiles of *at-rest* 2π kinks (*antikinks*) described by Eq. (20) as the initial data for the evolution. These profiles have been found numerically by solving Eq. (27) with boundary conditions (28). Then these 2π kinks (*antikinks*) have been provided with some velocity v . It has been observed that if μ is small enough, the kinks continue the motion emitting the radiation and can move for a long distances. At the same time the numerical experiments show that if μ is large, the 2π kinks lose the mobility conforming the results of Sec. III A.

The results of the numerical simulations of fluxon motion for three different values of nonlocality parameter μ and for the value of $\beta = 1$ are represented in Fig. 2. It follows from Fig. 2 that for $\mu = 3$ the fluxon moves with constant velocity but its motion is accompanied by plasma oscillations [Fig. 2 (panel a)]. Such a situation is typical of traditional Josephson

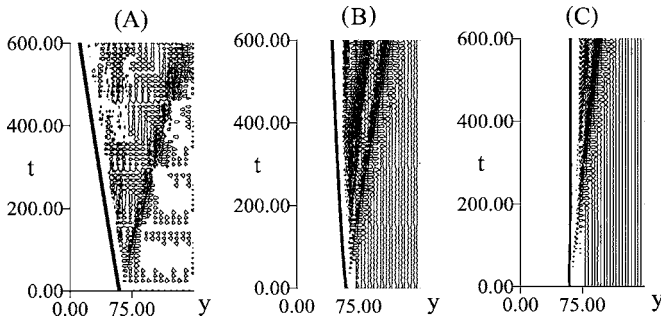


FIG. 2. Contour plots illustrating the motion of 2π kink. The initial kink profiles correspond to at-rest 2π -kink profiles [the solution of Eq. (20)]; the initial velocity is $v=0.1$. Kink moves from right to left; the bold lines in the figures are the lines of motion of the kink front. The pattern to the right of the bold line corresponds to the radiation which propagate backward. (a) $\mu=3$, $\beta=1$, the bold line is inclined and nearly straight that corresponds to uniform motion of the kink; (b) $\mu=5$, $\beta=1$, the kink motion is not uniform; and (c) $\mu=7$, $\beta=1$, kink remains motionless, extra energy transforms into radiation.

electrodynamics. As μ grows [Fig. 2(b)] the part of the energy emitted by plasma oscillations also grows and this leads to fluxon braking. At $\mu=7$ all the kinetic energy of the fluxon transforms into the plasma oscillations and the fluxon completely loses the mobility [Fig. 2(c)].

C. Interactions of kinks

Now let us turn to the question of how the variation of parameters μ and β affects solitonic properties of the fluxons. For this purpose we simulated the collisions of 2π kinks and antikinks described by Eq. (20). Again, we have used the profiles of at-rest 2π kink (antikink) described by Eq. (20) for the initial data. Initially, these profiles have been placed at some distance from each other. Then both the kink and the antikink have been provided with the velocities that are equal in modulus and directed toward each other. We observed that, in general, if β , μ , and the velocity v are not too large, two types of behavior after the collision have been observed:

(i) In some range of parameters μ and β the kink and antikink restore (approximately, up to some ripple) the shape after the interaction (see Fig. 3). It was natural to expect such a solitonic behavior in the limit cases (a) and (b) mentioned in Sec. III B, since in these cases the model under consideration is close to the sine-Gordon model. However, it turns out that the kinks and antikinks of Eq. (20) reveal soliton properties not only in the two limit cases but in the wider range of parameters. We observed that this kind of interaction takes place if the starting velocity v of the kink and the antikink is not too large, but it is greater than some critical value v_2 that depends on μ and β .

(ii) Another possibility is *binding* of the kink and antikink and *the forming of some localized long-lived pulsating object*, similar to the breather of the sine-Gordon equation (see Fig. 3). This object has a well-pronounced basic period. Sometimes, in addition to this period, it may have amplitude modulations of a greater period or stochastic amplitude

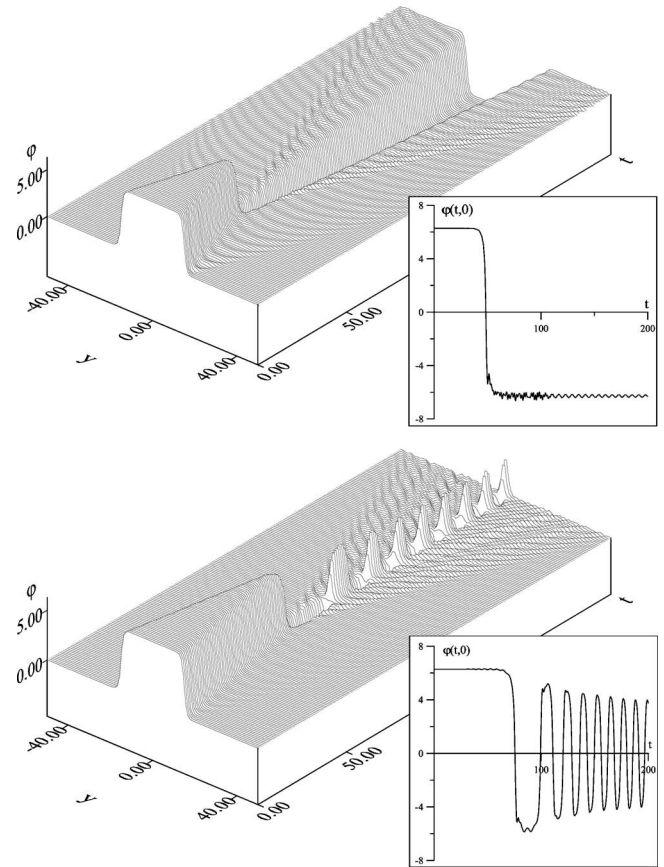


FIG. 3. Collision of 2π kink and 2π antikink for $\mu=1$, $\beta=0.5$ and the kink/antikink velocities equal $v=0.4$ (upper panel) and $v=0.2$ (lower panel).

modulations. This creation of a breather-like entity takes place if the starting velocity of the kink and antikink lies within the interval $0 < v < v_1$, where v_1 is another critical value depending on μ and β . More detailed discussion of these breather-like objects for Eq. (20) can be found in Sec. IV.

The diagram in Fig. 4 is calculated for $\mu=1$ and exhibits the regions on the plane (β, v) with different behavior after the kink-antikink collision. It shows that if the initial kinetic energy of kink and antikink is large enough, it covers the loss of energy by radiation that accompanies the collision of kink-antikink pair in a nonintegrable system. In this case kink and antikink restores their shapes after the collision. The threshold velocity v_2 for the solitonic behavior grows when the system moves away from sine-Gordon limit $\beta \ll 1$. One can observe that there is a gap between the values v_2 and v_1 . This gap is filled with alternating layers, ones where the interaction is solitonic and others where a pulsating bound state emerges. This situation is similar to one discovered for the ϕ^4 equation and described in Ref. 34.

As one of the parameters μ , β grows more, another type of the behavior can appear. In some cases we observed repulsion of the kink and the antikink without passing through each other. Also, in some other cases kink-antikink collision results in chaotic oscillation without any regular structure.

IV. NONLINEAR PLASMA OSCILLATIONS (AKIN BREATHERS) IN THE DISTRIBUTED JOSEPHSON JUNCTIONS WITH NONLOCAL ELECTRODYNAMICS

In the limit of local electrostatics nonlinear plasma oscillation of breather type correspond to exact solutions of the sine-Gordon equation.²⁹ The results of the simulations of kink-antikink interactions described above allow us to suppose that the nonlocal model under consideration also admits some class of breather-like excitations. These objects merit a separate analysis. They can be treated as *localized in space* and *periodic in time* solutions of Eq. (20) such that

$$\varphi(t,y) \rightarrow 0, \quad y \rightarrow \pm \infty,$$

$$\varphi(t,y) = \varphi\left(y, t + \frac{2\pi}{\omega}\right),$$

where $2\pi/\omega$ is the period of oscillations. Due to periodicity, these solutions can be thought of a Fourier series with respect to t . Moreover, since the nonlinearity is odd, Eq. (20) admits a specific class of periodic solutions such that their Fourier expansions include odd cosine terms only:

$$\varphi(t,y) = \sum_{n=0}^{\infty} \varphi_{2n+1}(y) \cos(2n+1)\omega t. \quad (31)$$

Assuming the form (31) for the desired breather-like solution and substituting it into Eq. (20), we obtain the following infinite system of nonlocal equations for the harmonics $\varphi_n(y)$:

$$\begin{aligned} L_{\mu,\beta} \left(\frac{d\varphi_1}{dy} \right) - (1 - \omega^2)\varphi_1 &= F_1(\varphi_1, \varphi_3, \dots); \\ L_{\mu,\beta} \left(\frac{d\varphi_3}{dy} \right) - (1 - 9\omega^2)\varphi_3 &= F_3(\varphi_1, \varphi_3, \dots); \\ &\vdots \\ L_{\mu,\beta} \left(\frac{d\varphi_{2n+1}}{dy} \right) - [1 - (2n+1)^2\omega^2]\varphi_{2n+1} &= F_{2n+1}(\varphi_1, \varphi_3, \dots); \\ &\vdots \end{aligned} \quad (32)$$

where $F_{2m+1}(\varphi_1, \varphi_3, \dots)$ is the coefficient in front of $\cos(2m+1)\omega t$ in the Fourier expansion of the nonlinearity $\sin[\sum_n \varphi_{2n+1}(y) \cos(2n+1)\omega t]$. The solutions to the finite systems obtained by truncating (32) can be taken as approximations of the desired solution. It is well known that, in some cases, even a single harmonic $\varphi_1(y)$ provides a good approximation for $\varphi(t,y)$. This approach sometimes called *rotating wave approximation*³⁵ was successfully used to construct discrete breathers in nonlinear lattices,^{35,36} radial breather-like states of the multidimensional sine-Gordon equation^{37,38} and fractional sine-Gordon equation,^{39,40} gap solitons,⁴¹ and other nonlinear problems.

Restricting the consideration to the case of a single harmonic,

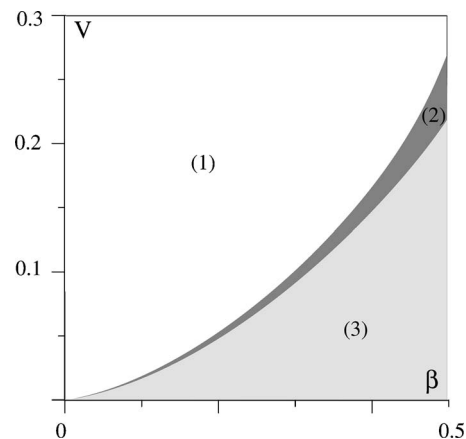


FIG. 4. The regions on the plane (β, v) where (1) the interactions between 2π kink and antikink result in oscillating bound state; (3) their interactions are of solitonic type; and (2) a intermediate layered region where either of the two types of the interaction may occur.

$$\varphi(t,y) \sim \varphi_1(y) \cos \omega t, \quad (33)$$

we obtain the equation

$$L_{\mu,\beta} \left(\frac{d\varphi_1}{dy} \right) + \omega^2 \varphi_1 - 2J_1(\varphi_1) = 0, \quad (34)$$

where $J_1(\xi)$ is the Bessel function. Equation (34) was solved numerically. The profiles of the solutions of Eq. (34) for various values of ω are represented in Fig. 5(a). Figure 5(b) exhibits how the amplitude of $\varphi_1(y)$ depends on ω . It appears that as ω tends to unity, the amplitude of $\varphi_1(y)$ tends to zero. Numerical solution of Eq. (20) under the initial conditions $\varphi(0,y) = \varphi_1(y)$, $\varphi_t(0,y) = 0$ shows that for some interval of ω adjacent to 1 the temporal evolution of the spatial profile is quite close to periodic (see Fig. 6).

Let us turn now to more detailed analysis of the situation. Consider the temporal evolution $\varphi(t,y)$ at $y=0$. Let $t=t_0$ and $t=t_1$ be the points of two consecutive maxima of the function $\varphi(t,0)$. At the point $t=t_1$ we define the value $\tilde{\omega}(t_1) \equiv 2\pi/(t_1 - t_0)$; for our analysis this value can be regarded as the “current” value of frequency. In particular, if $\varphi(t,0)$ is exactly periodic with the frequency ω and it has a single maximum point on the period, then $\tilde{\omega} = \omega$ for any point of maximum. Let us associate each point of maximum $t=t_k$ of $\varphi(t,0)$ with the point on the plane $(\varphi; \tilde{\omega})$ with coordinates $(\varphi(t_k, 0); \tilde{\omega}(t_k))$. So, $\varphi(t,0)$ can be characterized by a sequence of points on the plane $(\varphi; \tilde{\omega})$. We denote this sequence by T_φ .

At first we consider the sequences T_φ constructed for the initial data given by one harmonic approximation. We observed that at the first cycle of oscillations *some jump of the amplitude occurs*. This fact is associated with the generation of higher temporal harmonics (specifically, third and fifth ones), which can be distinguished in the temporal Fourier spectrum. The greater the amplitude of the initial profile is, the greater is the jump of the amplitude at the first cycle; if ω is close to 1, this jump is small, since higher harmonics are

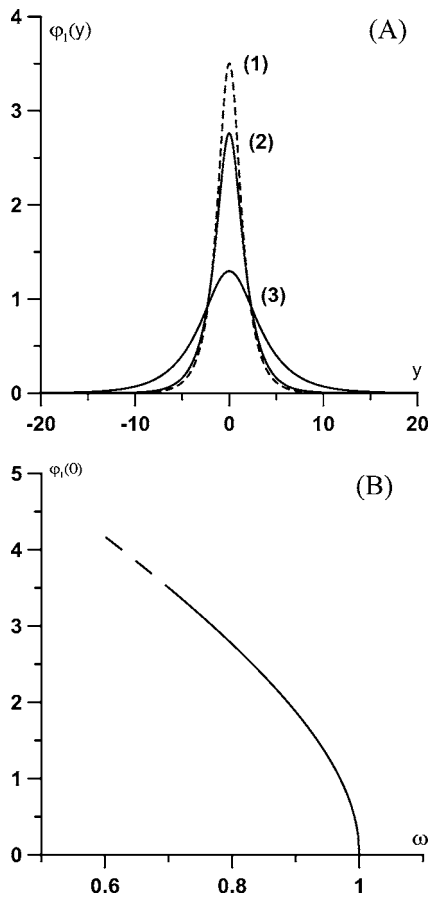


FIG. 5. (a) The graphs of $\varphi(y)$ for $\mu=1, \beta=1$ and $\omega=0.7$ (graph 1); $\omega=0.8$ (graph 2); $\omega=0.95$ (graph 3); (b) The graph of the amplitude $\varphi(0)$ versus ω for $\mu=1$ and $\beta=1$.

negligible. The sequence T_φ for the initial data given by one harmonic approximation $\omega=0.75$ is shown in Fig. 7 (gray points marked by the number 3).

Then, the amplitude of oscillation smoothly decreases. This fact is associated with losing energy through the radiation. This process becomes slower with time. For $\omega=0.7$ the amplitude falls from 3.38 to 3.16 for 750 temporal units; simultaneously the value $\tilde{\omega}$ grows from 0.69 to 0.72. The sequence T_φ for $\omega=0.75$ shown in Fig. 7 also is not a point

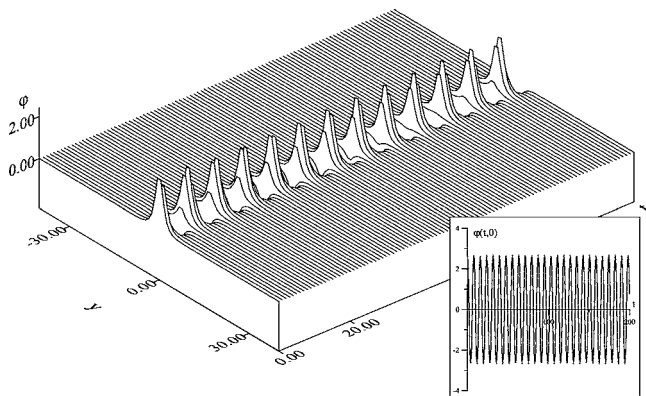


FIG. 6. The evolution of the initial profile given by the first harmonics $\varphi_1(y)$, $\omega=0.8$.

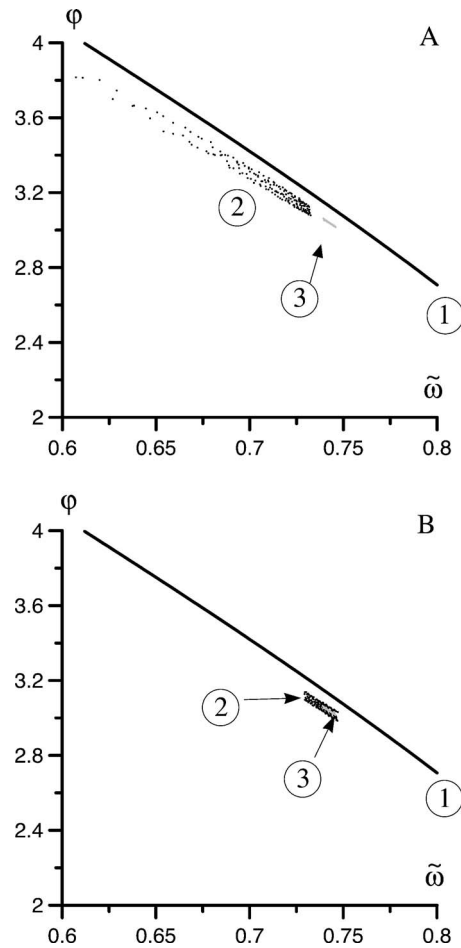


FIG. 7. The sequence T_φ (see the description in the text) corresponding to the kink-antikink collision depicted in Fig. 3 (black points, marked by the number 2) and the sequence T_φ for the initial profile given by one-harmonic approximation, $\omega=0.75$, 730 temporal units (gray points marked by the number 3). The initial velocity of kink and antikink is $v=0.2, \mu=1, \beta=0.5$. (a) The first 170 points of the sequence T_φ for kink-antikink collision; (b) Next 170 points of the same sequence. The curve marked by (1) is the dependence of the amplitude $\varphi(0)$ versus ω , a segment of the curve given in Fig. 5(b).

but seems like a segment of a curve. However, for the profiles corresponding to $0.8 \leq \omega \leq 1$ the amplitude of the oscillations and the value $\tilde{\omega}$ change very slowly, so the oscillations can be regarded (for the physical applications) as periodic ones.

Figure 7 exhibits the sequence T_φ corresponding to the kink-antikink collision depicted in Fig. 3 (right panel). The simulation has been fulfilled until $t=3000$. It follows from Fig. 7 that the points of T_φ approach the zone of the $(\varphi; \tilde{\omega})$ plane, where the periodic oscillations have been found. It follows from the figure that long-time simulation results in the “settling down” to the breather-like oscillations corresponding to $\omega \approx 0.75$.

The analysis given above does not imply that the oscillatory object that has been found corresponds to the *exact* breather solution of Eq. (20) i.e., is exactly spatially localized and periodic in time. We believe that after some time

this oscillatory state should decay due to the presence of higher harmonics, which can be delocalized. However, the lifetime of this entity can be very large, as this takes place in the famous problem on a breather in the ϕ^4 -model^{42,43} or on the radial breather for the 2D and 3D sine-Gordon equation^{37,38} where it runs to thousands of time units.

V. SUMMARY

To conclude, we have studied the electrodynamics of a nonlocal superconductive junction without dissipation and with electrodes of arbitrary thickness. The results of this study can be summarized as follows:

(i) The electrodynamics of the Josephson junction can be described by the nonlocal equation (20) if characteristic frequencies of the fields and currents in the junctions are not too high. There are two limits when this model becomes local. One of them corresponds to traditional electrodynamics when $\lambda_L \ll \lambda_J$. Another one corresponds to the junctions with thin electrodes, $d \ll \lambda_L$.

(ii) Involving nonlocality results in a change of dynamical properties of fluxons. Specifically, if the nonlocality is weak, fluxons conserve restricted mobility whereas if the nonlocality is strong they cannot move and remain fixed.

(iii) In both the limit cases mentioned in (i) the interactions between fluxons are of solitonic type. Moreover, they are solitonic in a wider region of parameters if the velocities of fluxons are greater than some threshold velocity. If the velocities of fluxons lie below another threshold value, their interaction results in creation of a long-lived oscillating state of breather type. Between these two threshold values the interaction can be both solitonic and nonsolitonic. Both the threshold values of velocity depend on physical and geometric parameters of the junction. Specifically, both these critical velocities grow if the thickness of the leads or the nonlocality parameter $\mu = \lambda_L / \lambda_J$ increases.

(iv) The nonlinear oscillations of breather type mentioned in (iii) are quite robust, long lived, and arise as a result of the evolution of initial states which have no instilled semblance to the “breather” forms that eventually emerged. Another pe-

culiarity of these entities is that they can be described well by one harmonic of temporal Fourier expansion.

Let us make some comments to these results. *First*, the drastic reduction of fluxon mobility when the parameter of nonlocality grows can result in an increase of the critical currents corresponding to the vortex motion. This phenomenon can occur in both artificially fabricated Josephson junction and granulated superconductor. *Second*, the emission of plasma oscillations observed in our numerical experiments which accompanies moving fluxon can result in amplification of the noise component of the signal in the current-voltage characteristic. The radiation of the moving fluxon in nonlocal Josephson electrodynamics has been discussed before^{25,44,45} and recently has been observed experimentally in a narrow Josephson junction described also by similar nonlocal equation.⁴⁶ The excitation of Cherenkov resonant plasma oscillations by a moving vortex leads to additional current steps on the current-voltage characteristics of the distributed Josephson junction with nonlocal electrodynamics. The generation of long-lived large amplitude oscillations of breather type, which can appear under the collisions of vortices moving in opposite directions in the junction, may also result in the volt-ampere characteristics. *Third*, in the nonlocal case, in the absence of moving single-quantum fluxons, the role of multi-quantum vortices (corresponding to 4π kinks, 6π kinks etc.) in the magnetic field transport increases. It is known that these entities can travel in nonlocal Josephson junction^{23,47,48} with high velocities and their contribution to current-voltage characteristics in the nonlocal model should be much more important in the nonlocal electrodynamics.

ACKNOWLEDGMENTS

The authors are grateful to T. Pierantozzi for help in the development of software for numerical simulations and to L. Vazquez for useful discussions. Also the authors thank V. P. Silin, Yu. M. Aliev, A. S. Malishevskii, and S. A. Uryupin for valuable comments and for indicating useful references. The work of G.A. has been supported by the Presidential Program in Support for Leading Scientific Schools.

¹Y. M. Ivanchenko and T. K. Soboleva, Phys. Lett. A **147**, 65 (1990).

²A. Gurevich, Phys. Rev. B **46**, R3187 (1992).

³A. Gurevich, Phys. Rev. B **48**, 12857 (1993).

⁴Yu. M. Aliev, V. P. Silin, and S. A. Uryupin, Supercond., Phys. Chem. Technol. **5**, 228 (1992).

⁵Yu. M. Aliev and V. P. Silin, J. Exp. Theor. Phys. **77**, 142 (1993).

⁶R. G. Mints and I. B. Shapiro, Phys. Rev. B **49**, 6188 (1994).

⁷Y. E. Kuzovlev and A. I. Lomtev, J. Exp. Theor. Phys. **84**, 986 (1997).

⁸N. Gronbech-Jensen and M. R. Samuelsen, Phys. Rev. Lett. **74**, 170 (1994).

⁹N. Gronbech-Jensen and M. R. Samuelsen, Phys. Rev. B **65**, 144512 (2002).

¹⁰Yu. M. Ivanchenko, Phys. Rev. B **52**, 79 (1995).

¹¹A. A. Abdumalikov, V. V. Kurin, C. Helm, A. De Col, Y. Koval, and A. V. Ustinov, arXiv: cond-mat/0411573.

¹²R. Gross, P. Chaudhari, D. Dimos, A. Gupta, and G. Koren, Phys. Rev. Lett. **64**, 228 (1990).

¹³A. Gurevich, M. S. Rzchowski, G. Daniels, S. Patnaik, B. M. Hinaus, F. Carillo, F. Tafuri, and D. C. Larbalestier, Phys. Rev. Lett. **88**, 097001 (2002).

¹⁴S. E. Russek, D. K. Lathrop, and B. Moeckly, Appl. Phys. Lett. **57**, 1155 (1990); G. Hammerl, A. Schmehl, R. R. Shultz, B. Goetz, H. Bielfeldt, C. W. Schneider, H. Hilgenkamp, and J. Mannhart, Nature (London) **407**, 162 (2000).

¹⁵A. Gurevich, Phys. Rev. B **65**, 214531 (2002).

¹⁶V. P. Silin, JETP Lett. **58**, 401 (1993).

- ¹⁷C. C. Tsuei and J. R. Kirtley, *Rev. Mod. Phys.* **72**, 969 (2000).
- ¹⁸Y. Tanaka and S. Kashiwaya, *Phys. Rev. B* **53**, R11957 (1996).
- ¹⁹Y. Tanaka and S. Kashiwaya, *Phys. Rev. B* **56**, 892 (1997).
- ²⁰D. A. Wollman, D. J. Van Harlingen, J. Giapintzakis, and D. M. Ginsberg, *Phys. Rev. Lett.* **74**, 797 (1995).
- ²¹L. Alff, A. Beck, R. Gross, A. Marx, S. Kleefisch, Th. Bauch, H. Sato, M. Naito, and G. Koren, *Phys. Rev. B* **58**, 11197 (1998).
- ²²G. L. Alfimov and A. F. Popkov, *Phys. Rev. B* **52**, 4503 (1995).
- ²³Yu. M. Aliev and V. P. Silin, *Phys. Lett. A* **177**, 259 (1993).
- ²⁴G. L. Alfimov and V. P. Silin, *J. Exp. Theor. Phys.* **79**, 369 (1994).
- ²⁵R. G. Mints and I. B. Snapiro, *Phys. Rev. B* **52**, 9691 (1995).
- ²⁶G. L. Alfimov, V. M. Eleonsky, and L. M. Lerman, *Chaos* **8**, 257 (1998).
- ²⁷G. L. Alfimov and V. P. Silin, *J. Exp. Theor. Phys.* **81**, 915 (1995).
- ²⁸A. C. Scott, F. Y. F. Chu, and D. W. McLaughlin, *Proc. IEEE*, **61** 1443 (1973); *Solitons and Condensed Matter Physics*, edited by A. Bishop and T. Schneider (Springer, Berlin, 1978), Vol. 8; R. D. Parmentier, in *Solitons in Action*, edited by K. Longren and A. Scott (Academic, New York, 1978), p. 173.
- ²⁹R. K. Dodd, J. C. Eilbeck, J. D. Gibbon, and H. C. Morris, *Solitons and Nonlinear Wave Equations* (Academic, New York, 1983).
- ³⁰P. Leiderer, J. Boneberg, P. Brull, V. Bujok, and S. Herminghaus, *Phys. Rev. Lett.* **71**, 2646 (1993); U. Bolz, D. Schmidt, B. Biehler, B.-U. Runge, R. G. Mints, K. Numessen, H. Kinder, and P. Leiderer, *Physica C* **388**, 715 (2003).
- ³¹Z. D. Genchev, *Supercond. Sci. Technol.* **10**, 543 (1997).
- ³²K. N. Ovchinnikov, V. P. Silin, and S. A. Uryupin, *Phys. Met. Metallogr.* **83**, 468 (1997).
- ³³A. S. Malishevskii, V. P. Silin, and S. A. Uryupin, *Phys. Solid State*, **41** (7), 1160 (1999).
- ³⁴D. K. Campbell, J. F. Schonfeld, and C. A. Wingate, *Physica D* **9**, 1 (1983).
- ³⁵S. Flach and C. R. Willis, *Phys. Rep.*, **295**, 181 (1998).
- ³⁶T. Bountis, H. W. Capel, M. Kollmann, J. C. Ross, J. M. Bergamin, and J. P. Van der Weele, *Phys. Lett. A* **268**, 50 (2000).
- ³⁷B. Piette and W. J. Zakrzewski, *Nonlinearity* **11**, 1103 (1998).
- ³⁸G. L. Alfimov, W. A. B. Evans, and L. Vázquez, *Nonlinearity*, **13**, 1657 (2000).
- ³⁹G. Alfimov, T. Pierantozzi, and L. Vázquez, “Numerical study of a nonlocal sine-Gordon equation,” in *Nonlinear Waves: Classical and Quantum Aspects*, edited by F. Kh. Abdullaev and V. V. Konotop, NATO Science Series, Vol. 153, p. 121, Proceedings of the Workshop in Estoril, Portugal, 13–17 July, 2003 (Kluwer Academic, Dordrecht, 2003).
- ⁴⁰G. Alfimov, T. Pierantozzi, and L. Vázquez, “Numerical study of a fractional sine-Gordon equation, in *Fractional Differentiation And its Applications*, edited by A. Le Mahaute, J. A. Tenreiro Machado, J. C. Trigeassou, and J. Sabatier, (UBooks Verlag, Neusäß, 2006 pp. 153–162).
- ⁴¹G. Alfimov and V. Konotop, *Physica D* **146**, p 307 (2000).
- ⁴²H. Segur and M. D. Kruskal, *Phys. Rev. Lett.* **58**, 747 (1987).
- ⁴³J. P. Boyd, *Nonlinearity* **3**, 177 (1990).
- ⁴⁴V. P. Silin and A. V. Studenov, *Phys. Solid State* **39**, 384 (1997).
- ⁴⁵A. S. Malishevskii, V. P. Silin, S. A. Uryupin, and S. G. Uspenskii, *Phys. Lett. A* **348**, 361 (2006).
- ⁴⁶A. A. Abdumalikov, M. V. Fistul, and A. V. Ustinov, *Phys. Rev. B* **72**, 144526 (2005).
- ⁴⁷V. P. Silin and A. V. Studenov, *Phys. Lett. A* **264**, 324 (1999).
- ⁴⁸A. S. Malishevskii, V. P. Silin, and S. A. Uryupin, *Phys. Solid State* **43**, 1 (2001).